ESC European Society of Cardiology

European Heart Journal - Digital Health (2022) **3**, 505–515
https://doi.org/10.1093/ehjdh/ztac050

ORIGINAL ARTICLE

Non-hyperaemic assessment of coronary ischaemia: application of machine learning techniques

James N. Cameron [1,*,†], Andrea Comella[2,†], Nigel Sutherland[1], Adam J. Brown[3], and Thanh G. Phan[4]

[1]Department of Cardiology, Northern Hospital Melbourne, 185 Cooper St, Epping, VIC 3076, Australia; [2]Alfred Hospital, Melbourne 3004, Australia; [3]Monash Cardiovascular Research Centre, MonashHeart, Monash Health, Melbourne 3168, Australia; and [4]Department of Neurology, Monash Health and School of Clinical Sciences at Monash Health, Monash University, Melbourne 3168, Australia

Received 12 June 2022; revised 24 July 2022; online publish-ahead-of-print 14 September 2022

Aims Hyperaemic and non-hyperaemic pressure ratios (NHPR) are routinely used to identify significant coronary lesions. Machine learning (ML) techniques may help better understand these indices and guide future practice. This study assessed the ability of a purpose-built ML algorithm to classify coronary ischaemia during non-hyperaemia compared with the existing gold-standard technique (fractional flow reserve, FFR). Further, it investigated whether ML could identify components of coronary and aortic pressure cycles indicative of ischaemia.

Methods and results Seventy-seven coronary vessel lesions (39 FFR defined ischaemia, 53 patients) with proximal and distal non-hyperaemic pressure waveforms and FFR values were assessed using supervised and unsupervised learning techniques in combination with principal component analysis (PCA). Fractional flow reserve measurements were obtained from the right coronary artery (13), left anterior descending (46), left circumflex (11), left main (1), obtuse marginal (2), and diagonal (4). The most accurate supervised learning classification utilized whole-cycle aortic with diastolic distal blood pressure waveforms, yielding a classification accuracy of 86.9% (sensitivity 86.8%, specificity 87.2%, positive predictive value 86.8%, negative predictive value 87.2%). Principal component analysis showed subtle variations in coronary pressures at the start of diastole have significant relation to ischaemia, and whole-cycle aortic pressure data are important for determining ischaemia.

Conclusions Our ML algorithm classifies significant coronary lesions with accuracy similar to previous studies comparing time-domain NHPRs with FFR. Further, it has identified characteristics of pressure waveforms that relate to function. These results provide an application of ML to ischaemia requiring only standard data from non-hyperaemic pressure measurements.

* Corresponding author. Tel: +61 (03) 8405 8000, Email: jamescameron91@gmail.com
†These authors contributed equally to this work.

Graphical Abstract

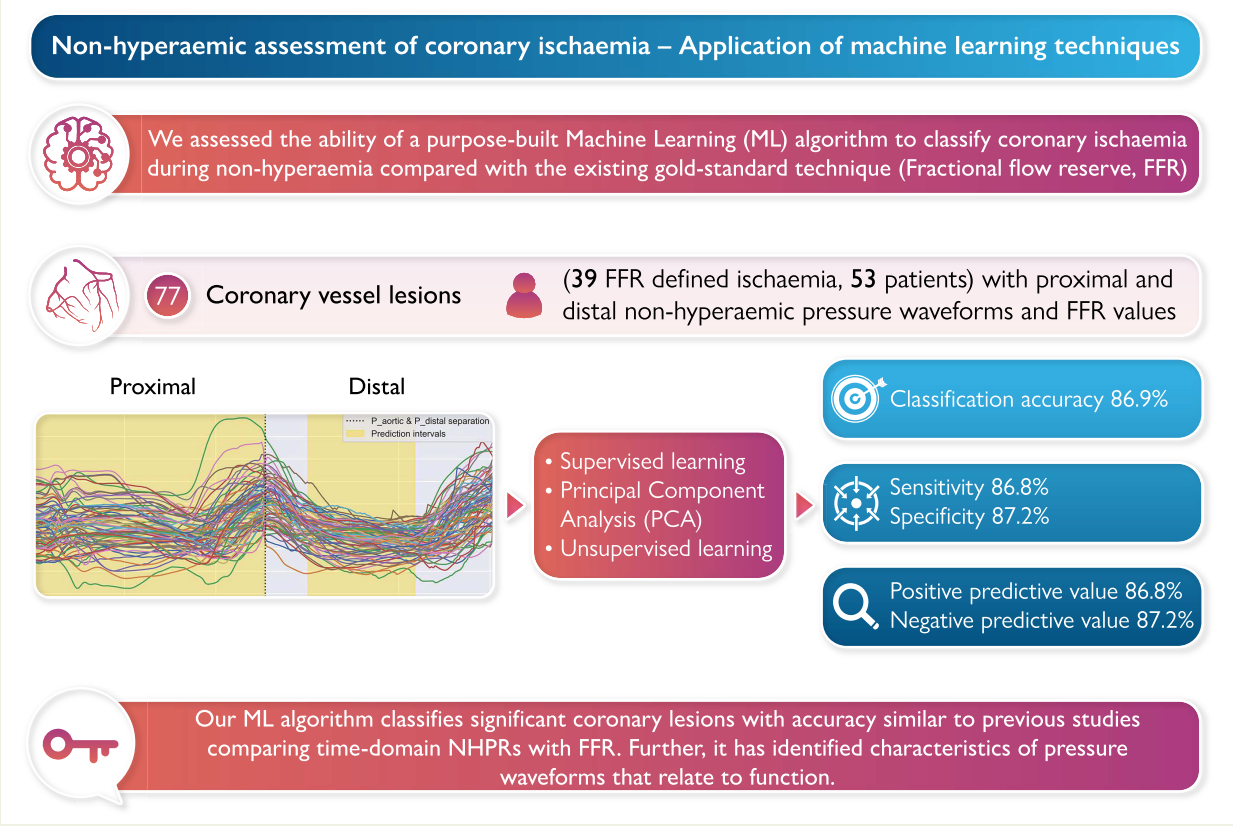

Applying machine learning to classify significant coronary ischaemia using non-hyperaemic pressure waveforms. Inputs are modifiable intervals of coronary pressure waveforms, outputting sensitivity, specificity, negative predictive value, positive predictive value, and overall classification accuracy in the form of a confusion matrix. Principal component analysis was used to investigate what segments of the pressure waveforms contain characteristics associated with ischaemia.

Keywords Machine learning • Ischaemia • Non-hyperaemia • Fractional flow reserve

Introduction

Myocardial ischaemia is defined as an inadequate oxygen supply at the cellular level to provide for the required respiration of myocytes. This is predominantly caused by epicardial coronary artery obstruction limiting adequate blood flow to the myocardium, and in stable coronary artery disease, is manifest by an inability to increase coronary blood flow in response to increased tissue demand. Identification of ischaemia secondary to coronary artery lesions is the basis of guideline supported management of coronary artery disease. Coronary angiography allows visual assessment of atheroma severity within coronary vessels, with flow or pressure-based measurements recommended in assessing their significance.[1]

In any fluid, pressure (force per unit area or energy per unit volume) relates to the ability of the fluid to perform work. Blood pressure can be interpreted as the transfer of mechanical energy from contracting cardiac myocytes to circulating blood, producing flow through the systemic vasculature, and delivering oxygen to tissues. While it is recognized that the direct measurement of coronary flow provides a more physiologic assessment of cardiac ischaemia (since volumetric flux at a given oxygen saturation equates to actual oxygen supply), the practical ease of coronary artery pressure measurement, combined with the difficulties of capturing accurate coronary flow in clinical practice, has given prominence to pressure-based indices.

Ratios of distal to proximal coronary artery pressure [$P_{(distal)}$/$P_{(aortic)}$] dominate clinical application, with various hyperaemic and non-hyperaemic indices incorporating specific intervals of the cardiac pressure cycle. These indices, whether calculated over the entire cycle, the physiologically identified wave-free period or incorporating all or specific algorithmically determined points in diastole have all proven to provide remarkably similar clinical utility.[2–5]

Invasively measured fractional flow reserve (FFR) is a well-established and guideline recommended standard of care for the assessment of intermediate grade stenosis, which can be used to guide coronary revascularization.[1] Assessment of FFR requires the administration of a hyperaemic agent (typically adenosine) to induce hyperaemia and reduce coronary microvascular impedance in the volume

subtended by the epicardial coronary artery under investigation. Fractional flow reserve is associated with increased procedural cost and procedural risk, including bronchospasm, chest pain, dyspnoea, relative hypotension, and atrioventricular conduction delay compared with non-hyperaemic pressure ratios (NHPRs). For this reason, NHPRs have recently been developed and are available for routine clinical application.

The first NHPR approach proposed and subsequently extensively validated was the instantaneous wave-free ratio (iFR),[6] which utilized the identified wave-free interval within diastole to calculate an index of ischaemia, given by the ratio of the mean diastolic pressure during the wave-free period distal to the lesion (P_d) to the aortic pressure proximal to the lesion (P_a) during the same interval. Several commercial NHPR approaches employing various pressure intervals throughout the cardiac cycle have since been defined and have been accepted into clinical usage. All currently available NHPR metrics employ either whole-cycle calculations or varying features of the diastolic pressure waveform in their calculation.

In the various competing pressure-based ischaemic indices (hyperaemic and non-hyperaemic), the input is by necessity identical: a measured pressure waveform. Since it is impossible to add information content to empirical data by post-processing, it follows therefore that these various algorithmic approaches must vary only in their relative assumptions and the differing weights given to specific pressure waveform characteristics and features in the calculations applied. To infer flow deficiency based solely on pressure measurement, all currently available techniques utilize some form of approximation to linearize the relationship between pressure and flow and thus convert the complex-valued impedance into the better understood parameter of 'resistance'. It is these approximations and assumptions used to linearize the pressure–flow relationship where major differences in the pressure-based assessments of coronary ischaemia lie, and would be the basis of any clinically relevant and practical differences between the various indices proposed.

In view of the apparent robustness and practical similarity of results when NHPRs are compared, we sought to determine the ability of machine learning (ML) techniques to identify the presence of ischaemia in the myocardium subtended by a particular epicardial coronary artery, and further, to identify the features and components of coronary and aortic pressure cycles most associated with ischaemia, especially during resting conditions.

Methods

Machine learning and principal component analysis

A summary of the methodology used in this analysis is as follows, with an in-depth explanation provided in the Supplementary material online:

(1) A supervised learning algorithm was developed (*Figure 1*) using non-hyperaemic pressure waveforms and pre-assigned FFR ischaemic/non-ischaemic lesions to classify ischaemia in 'unseen' coronary vessels.
(2) Principal component analysis (PCA) was used independently to investigate what segments of the pressure waveforms contain characteristics associated with ischaemia (*Figure 2*), as well as a being an intermediary step in data pre-processing for both the supervised and unsupervised learning algorithms.
(3) Unsupervised learning using t-distributed stochastic neighbour embedding (t-SNE) reduced the multi-dimensional data to a two-dimensional plot (*Figures 3* and *4*) and attempted to learn characteristics of the pressure cycle as a function of time. A Gaussian mixture modelling (GMM) clustering algorithm investigated if meaningful clusters formed, and if clusters were representative of ischaemia.

The ML algorithms and data-analyses were performed using the open-source distribution of Anaconda's Python 3.9.6 (Release date June 28, 2021) and the scikit-learn library.

We utilized an established library consisting of 93 sets of aortic and intracoronary pressure cycles measured at a 100 Hz sampling rate, each representing a unique vessel. Fractional flow reserves were obtained using IV adenosine, and stenosis severity (*Table 1*) was defined by visual assessment at time of coronary angiogram. The number of pressure traces per patient ranged from 1 to the number of coronary arteries assessed. Poor quality tracings with ensemble-averaged pressure cycles showing large confidence intervals were removed from the analysis, resulting in a cohort of 77 ensemble-averaged pressure cycles made up of 1155 individual daughter pressure cycles.

Two distinct input methods were compared in the PCA and ML algorithms (see Supplementary material online, *Figure S1*):

(1) Ensemble-average method: 77 lesions represented by their averaged pressure waveform. Using this method, 77 pressure waveforms were used in the supervised learning algorithm, with the unsupervised t-SNE dimensionality reduction graphs having 77 points, 1 for each ensemble-averaged cycle.
(2) Individual 'daughter' cycle method: Each pressure waveform from the 77 lesions' first 15 daughter pressure cycles (non-overlapping) was treated as a unique data set (with the ischaemic label of each individual cycle inherited and assumed constant). Using this method, 1155 pressure waveforms were used in the supervised learning algorithm, with the unsupervised t-SNE dimensionality reduction graphs having 1155 points, 1 for each individual cycle.

All 77 ensemble-averaged and 1155 individual cycles were interpolated to the length of the longest individual cycle.

All data were standardized using *z*-score standardization, transforming the data onto a unit scale (mean = 0 and variance = 1). Two methods of *z*-score standardization were used in the PCA and ML algorithms to investigate whether ischaemia in coronary vessels based on FFR is affected by blood pressure, and if FFR should be interpreted as a function of absolute blood pressure. Inter-vessel standardization standardized the blood pressure of a single waveform (ensembled or individual 'daughter') using the entire dataset, compared with intra-vessel standardization's per lesion basis (see Supplementary material online, *Figure S2*):

(1) Intra-vessel standardization: $z = \frac{\text{Pressure} - \text{mean}_{\text{single lesion}}}{\text{standard deviation}_{\text{single lesion}}}$
(2) Inter-vessel standardization: $z = \frac{\text{Pressure} - \text{mean}_{\text{all lesions}}}{\text{standard deviation}_{\text{all lesions}}}$

Exemption from formal Human Research Ethics Committee review was obtained from Research Support Services, Monash Health.

Results

The 77 coronary pressure cycles (39 FFR defined ischaemia) represented a cohort of 53 patients (35.9% female) with a pooled mean age of 66.3 ± 10.6 years. Fractional flow reserve measurements

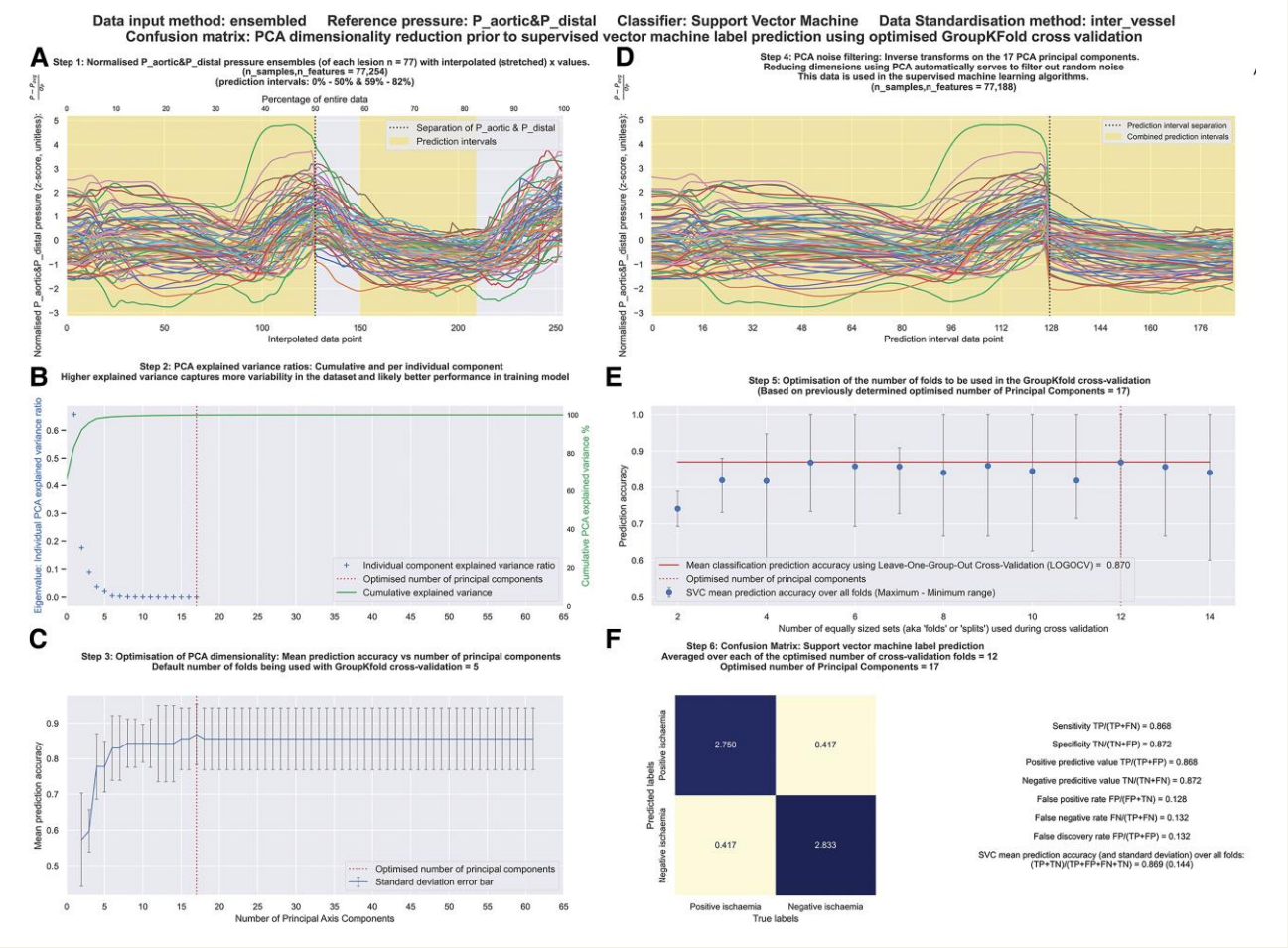

Figure 1 Stepwise representation of the supervised machine learning algorithm. Panels labelled *A–F* (Steps 1–6) display the ability of including/excluding different prediction intervals of the cardiac cycle. Data points to the left of the dashed black lines in Row 1 belong to whole-cycle $P_{(aortic)}$ data, with data points to the right belonging to the 18–64% prediction interval of $P_{(distal)}$. Optimized mean classification accuracy, sensitivity, specificity, positive predictive value, and negative predictive value are calculated using the confusion matrix in the bottom right panel. ML, machine learning; NPV, negative predictive value; PPV, positive predictive value.

were obtained from the right coronary artery (13), left anterior descending (46), left circumflex (11), left main (1), obtuse marginal (2), and diagonal (4). Characteristics (age, gender, coronary artery assessed, stenosis severity, and indication for coronary angiography) of the study population are given in *Table 1*. *Figure 5* shows the range of FFR values.

Supervised learning

Results using supervised learning to classify non-hyperaemic coronary ischaemia using whole-cycle non-hyperaemic data are summarized in *Table 2*. With inter-vessel standardization, the sensitivity, specificity, positive predictive values (PPV), and negative predictive values (NPV) based on ensemble-averaged, whole-cycle aortic, and distal pressure [$P_{(aortic\ and\ distal)}$] waveforms, was 84.2, 84.6, and 84.2, and 84.6%, respectively; with overall mean classification accuracy being 84.4% (standard deviation 15.3%). When individual (non-ensembled) $P_{(aortic\ and\ distal)}$ waveforms were used, the corresponding values were consistently lower at 74.7, 80.5, 78.9, and 76.6%, with an overall mean classification accuracy of 77.4% (standard deviation 19.1%).

Sensitivity, specificity, PPV, NPV, and overall accuracy using the derived signal $P_{(aortic–distal)}$ in the case of individual waveforms and inter-vessel standardization was 76.0, 76.8, 76.1, 76.6, and 76.4%, respectively. Using solely $P_{(aortic)}$ or $P_{(distal)}$ yielded inferior classification accuracies. As shown in *Table 2*, which compares whole-cycle data, classification accuracy was in all cases highest using $P_{(aortic\ and\ distal)}$ regardless of permutation.

Supervised learning was also employed using different periods of both the aortic distal pressure [$P_{(aortic\ and\ distal)}$] waveforms (adjusted 'prediction intervals', as shown by shading in panel 1 of *Figure 1*). *Table 3* summarizes these iterations, with highest classification accuracies found using prediction intervals of 0–100% (whole cycle) and 18–64% (interestingly approximating diastole) for the $P_{(aortic)}$ and $P_{(distal)}$ components. *Table 4* shows classification accuracies for $P_{(distal)}$ and $P_{(aortic–distal)}$ along with $P_{(aortic\ and\ distal)}$ using this 18–64% prediction interval. *Tables 2* and *4* compare incorporating whole-cycle data to instead this approximate diastolic portion only.

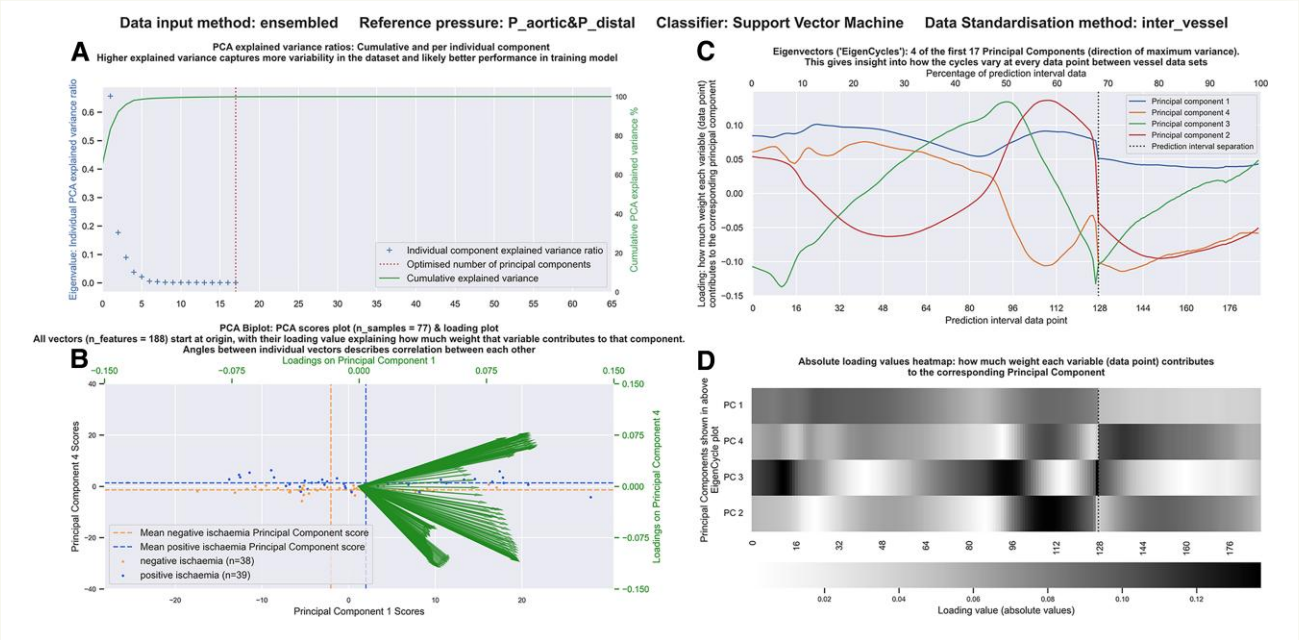

Figure 2 Principal component analysis biplot, 'EigenCycles' (Eigenvector) plot and loading values heatmap. The first four principal components in descending order of largest mean differences between positive and negative ischaemia principal component scores [$P_{(\text{aortic and distal})}$ data using inter-vessel standardization and whole-cycle $P_{(\text{aortic})}$ (0–100%) with the diastolic portion (18–64%) of $P_{(\text{distal})}$ waveforms]. The EigenCycles plot and loading values heatmap shown in Column 2 are alternate ways of presenting the Biplot information. Data points to the left of the dashed black lines in Column 2 belong to whole-cycle $P_{(\text{aortic})}$ data, with data points to the right belonging to the 18–64% prediction interval of $P_{(\text{distal})}$. PCA, principal component analysis.

Figure 1 illustrates the supervised learning algorithm generating the results shown in *Tables 2–4* to identify optimal data input conditions. Sensitivity, specificity, PPV, NPV using ensemble-averaged $P_{(\text{aortic and distal})}$ data and inter-vessel standardization incorporating the entire $P_{(\text{aortic})}$ (0–100%) waveform with an approximate diastolic portion (18–64%) of $P_{(\text{distal})}$ were 86.8, 87.2, 86.8, 87.2%, respectively, with an overall classification accuracy of 86.9%.

Principal component analysis

The PCA Biplot in *Figure 2* uses the identified optimal data input conditions and presents the principal component scores (PCS) for principal components (PC) 1 and 4 of each pressure waveform (those being the two PC found to have the largest separation in ischaemia classified by the ML algorithm). The vectors represent loading scores of each variable/dimension (pressure data point) in those two PC.

Each PC captures a given amount of variance from the entire data set (in descending order, most variance to least variance). A variable's loading score is a measure of how much that variable contributes towards that specific amount of variance in that specific PC. The PCS describes the coordinate location of each variable for a given PC axis, relative to the centre of the data. Principal component scores are representations of the original data when plotted on rotated PC axes.

PC 1 and PC 4 account for ~64 and 4% of explained variance, respectively (panel 2 in *Figure 1* and first panel in *Figure 2*). PC 1 best separated ischaemia, with data points belonging to whole-cycle $P_{(\text{aortic})}$ data contributing most to PC 1's explained variance (darkest shades in the absolute loading values heatmap) with greatest influence from data points 25–50 in keeping with beginning- to mid-diastole (panel 1 *Figure 1*). PC 4's largest absolute loading values were at the start of the 18–64% (approximate diastole) prediction interval of $P_{(\text{distal})}$ data (to the right of the dashed black line in Column 2). PC 3 and 2 accounted for 17 and 9% of total variance, respectively, and did not distinguish between ischaemic data as well as did PC 1 and 4. PC 3 and 2 had larger absolute loading values in certain intervals of the cardiac cycle (darkest shading on heatmap) compared with PC 1 and 4, implying a narrower range of values contributed more significantly to their individual overall explained variances. These intervals, approximately data points 0–18 for PC 3 (peak systolic pressure to approximate end of systole), and 90–100 and 100–120 for PC 3 and 4, respectively (start of systole and early- to mid-systole, respectively), likely contributed significantly in their ability to separate ischaemic and non-ischaemic data.

Unsupervised learning

Figures 3 and *4* are examples of unsupervised learning two-dimensional representations of the multi-dimensional pressure waveforms produced using t-SNE and GMM clustering, with ischaemic labels delineated by colour. *Figure 3* uses those conditions, which yielded a supervised learning classification accuracy of 86.9% as in *Table 3*, *Figure 4* shows results utilizing individual cycles and whole-cycle $P_{(\text{aortic–distal})}$ data. The GMM clusters shown in these figures, which model data as a collection of Gaussian blobs in a probabilistic model describing the distribution of the data, was not able to find distinct clusters or separate ischaemic from non-ischaemic data.

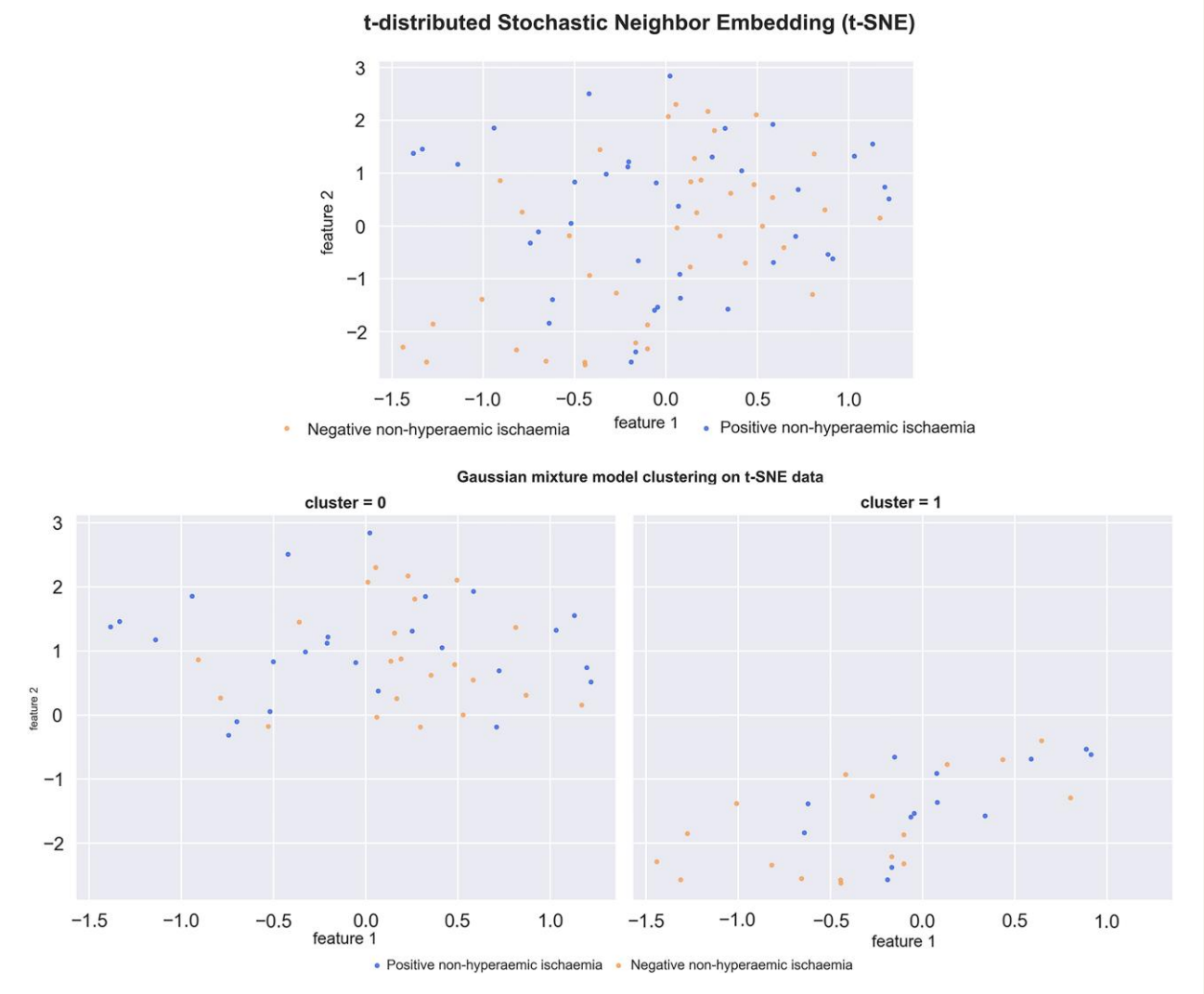

Figure 3 Unsupervised learning two-dimensional representations of multi-dimensional pressure waveforms produced using t-distributed stochastic neighbour embedding and Gaussian mixture modelling clustering. Using conditions, which yielded a supervised learning classification accuracy of 86.9% in *Table 3* [ensemble average, inter-vessel, $P_{(\text{aortic and distal})}$]. Ischaemic labels are delineated by colour. The Gaussian mixture modelling clusters shown in these figures, which model data as a collection of Gaussian blobs in a probabilistic model describing the distribution of the data, were not able to find distinct clusters or separate ischaemic from non-ischaemic data. GMM, Gaussian mixture modelling; t-SNE, t-distributed stochastic neighbour embedding.

Discussion

The principal findings of this study are (i) supervised ML techniques can accurately classify ischaemia producing coronary lesions (defined by FFR < 0.8), (ii) combining aortic and coronary pressure waveforms increases classification accuracy, (iii) inter-vessel standardization, which allows for influence of absolute blood pressure increases classification accuracy, (iv) there is a negligible difference between using ensembled-averaged or individual blood pressure waveforms, (v) PCA showed subtle variations in coronary pressures at the start of diastole as well as whole-cycle aortic pressure data are important in dictating ischaemia, with $P_{(\text{aortic})}$ heavily influencing systolic coronary perfusion, and (vi) unsupervised learning using t-SNE did not clearly partition ischaemic vs. non-ischaemic data in two-dimensions, nor did it show any clearly defined clustering of data.

There has been interest and debate regarding the practical and clinical benefits of NHPRs, as well as appropriateness of application of whole-cycle pressure waveform indices compared with those utilizing only specific diastolic segments. Most studies have demonstrated no practical difference between whole-cycle and diastole only calculations and have concluded that both approaches have clinical utility as compared with FFR.[2–5,7]

Multiple trials investigating iFR have shown 80–85% agreement with FFR (using thresholds of 0.89 and 0.80, respectively) in classifying lesions as haemodynamically significant.[6,8,9] In 2018 using primary endpoints of death from any cause; nonfatal myocardial infarction, and unplanned revascularization within 12 months in

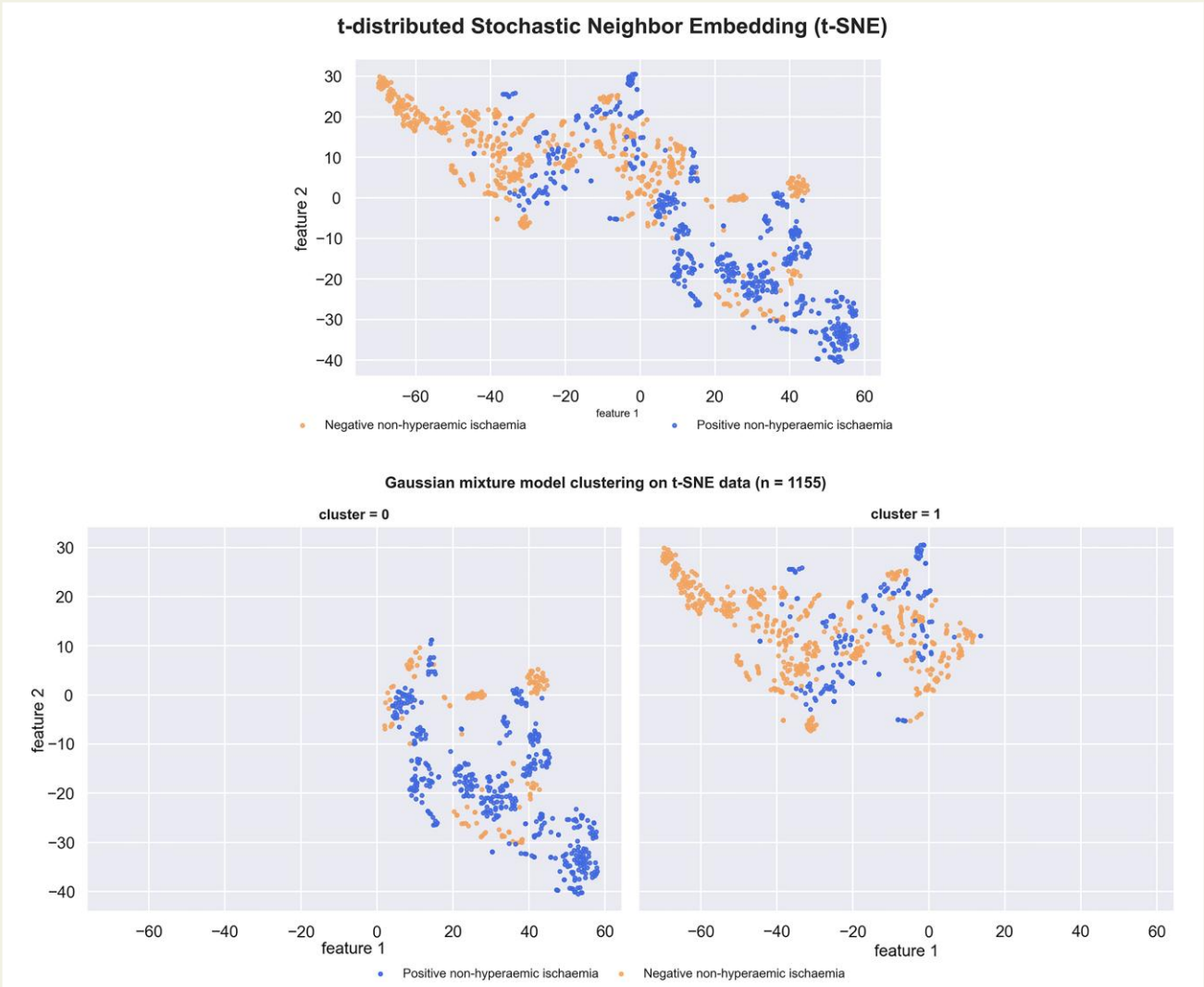

Figure 4 Unsupervised learning two-dimensional representations of multi-dimensional pressure waveforms produced using t-distributed stochastic neighbour embedding and Gaussian mixture modelling clustering. Comparison to *Figure 3* using instead the individual cycle method and $P_{(aortic–distal)}$ over the entire cycle (0–100% prediction interval). Ischaemic labels are delineated by colour. The Gaussian mixture modelling clusters shown in these figures, which model data as a collection of Gaussian blobs in a probabilistic model describing the distribution of the data, were not able to find distinct clusters or separate ischaemic from non-ischaemic data. GMM, Gaussian Mixture Modelling; t-SNE, t-distributed stochastic neighbour embedding.

patients with stable angina or an acute coronary syndrome, Götberg *et al.*[5] showed that iFR-guided revascularization was non-inferior to FFR-guided revascularization with respect to the rate of major adverse cardiac events at 12 months. In the 2018 VALIDATE resting full-cycle ratio (RFR) study, Svanerud *et al.*[4] showed diagnostic equivalence between RFR and iFR, and concordance between the 2 vs. FFR. Resting full-cycle ratio, iFR, and whole-cycle average $P_{(distal/aortic)}$ were correlated with FFR, with area under the receiver operating curves being almost identical for both RFR and iFR compared with FFR. Diagnostic accuracy of RFR compared with FFR was 81.3% with a sensitivity, specificity, PPV, and NPV of 71.5, 88.0, 80.6, and 81.6%, respectively. The corresponding values for iFR compared with FFR were 80.8, 69.3, 88.8, 81.1, and 80.6%, while for whole-cycle average $P_{(distal/aortic)}$ values were 81.4, 62.2, 94.8, 89.2, and 78.3%. Johnson *et al.*[3] further confirmed numerical equivalency among resting metrics to iFR, comparing dPR (diastolic pressure ratio), a metric based on a more complex algorithm relating diastolic to mean whole-cycle blood pressure, to iFR. Diagnostic accuracy of dPR compared with iFR was 92.2% with a sensitivity 87.7% and specificity of 95.9%. This is consistent to Svanerud *et al.*'s results comparing RFR to iFR (diagnostic accuracy 97.4%, sensitivity 98.2%, specificity 96.9%, PPV 94.5%, NPV 99.0%).

Our supervised ML algorithm's similar diagnostic accuracies (ranging from 78 to 87% when compared with FFR) are supportive of the likely comparability between ML techniques with iFR results. Supporting this conclusion are our previous results[7] in the specific case of severe aortic stenosis in which NHPRs including whole-cycle $P_{(distal/aortic)}$, diastolic pressure ratios (DPR and dPR) and diastolic

Table 1 Characteristics of study population

Age ± standard deviation (years)	66.3 ± 10.6
Gender (male/female)	39/14
Stenosis severity[a]	(Number of lesions)
Mild	16
Moderate	47
Severe	14
Indication for coronary assessment	(Number of patients)
Unstable angina	1
Stable coronary syndrome	44
Late presentation acute myocardial infarction (AMI)	1
Non-ST-elevation myocardial infarction (NSTEMI)	7
Coronary artery assessed (stenosis-mild, moderate, severe)	
Left anterior descending	46 (8,27,11)
Left circumflex	11 (4,7,0)
Left main	1 (1,0,0)
Obtuse marginal	2 (0,2,0)
Diagonal	4 (0,3,1)
Right coronary artery	13 (3,8,2)

[a]Stenosis severity: mild <50% area stenosis, moderate 50–70% area stenosis, severe >70% area stenosis by visual assessment at time of procedure.

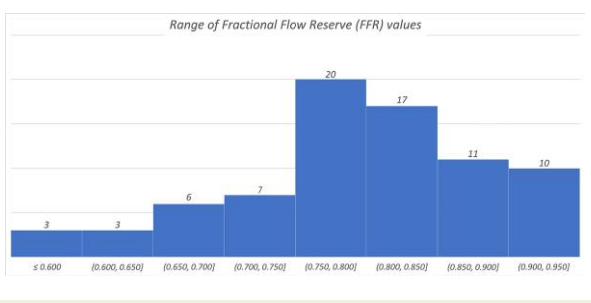

Figure 5 Range of fractional flow reserve values for the 77 coronary lesions. FFR, fractional flow reserve.

hyperaemia-free ratio all displayed strong correlation and diagnostic accuracies in the high ninety percent range compared with iFR.

It is worth highlighting the features of the ML system that appear relevant to these results. As expected, precision improved with combinations of $P_{(aortic)}$ and $P_{(distal)}$ [$P_{(aortic\ and\ distal)}$] when compared with either pressure waveform alone. Perhaps surprisingly, however, best precision was obtained when patient ensemble-averaged pressure waveform was utilized rather than a series of individual cycles. This is likely due to the ensembling process eliminating individual cycle noise and artefact and presenting the ML process with a more representative signal. Differences in precision between ensembled and individual cycles were small and may or may not be relevant in practice, for example in choosing how many cycles to base FFR calculations. Interestingly, highest accuracies were evident using

Table 2 Supervised learning ischaemic classification accuracies—using whole cardiac cycles

Number of pressure cycles	**15**																			
Classifier	**SVM**																			
Data input	**Ensemble-average method**								**Individual cycle method**											
Standardization method	**Intra-vessel**				**Inter-vessel**				**Intra-vessel**				**Inter-vessel**							
Reference pressure	P_{aortic}	P_{distal}	$P_{aortic-distal}$	$P_{aortic\ and\ distal}$	P_{aortic}	P_{distal}	$P_{aortic-distal}$	$P_{aortic\ and\ distal}$	P_{aortic}	P_{distal}	$P_{aortic-distal}$	$P_{aortic\ and\ distal}$	P_{aortic}	P_{distal}	$P_{aortic-distal}$	$P_{aortic\ and\ distal}$	P_{aortic}	P_{distal}	$P_{aortic-distal}$	$P_{aortic\ and\ distal}$
Aortic pressure prediction interval	0–100%	NA	0–100%	0–100%	0–100%	NA	0–100%	0–100%	0–100%	NA	0–100%	0–100%	0–100%	NA	0–100%	0–100%	0–100%	NA	0–100%	0–100%
Distal pressure prediction interval	NA	0–100%		0–100%	NA	0–100%		0–100%	NA	0–100%		0–100%	NA	0–100%		0–100%				
LOGOCV classification accuracy	51.9%	64.9%	67.5%	**77.9%**	58.4%	68.8%	74.0%	**84.4%**	57.0%	67.4%	66.8%	**78.7%**	59.9%	65.5%	76.5%	**77.7%**				
Optimized GroupKFold mean classification accuracy (standard deviation)	53.5% (18.4%)	64.9% (16.5%)	67.6% (3.5%)	**77.8% (10.0%)**	58.5% (16.7%)	68.8% (12.1%)	74.0% (10.2%)	**84.4%** (15.3%)	56.8% (11.8%)	67.2% (13.2%)	66.6% (11.0%)	**78.6% (8.3%)**	59.7% (7.9%)	65.1% (12.0%)	76.4% (11.1%)	**77.4% (19.1%)**				
Sensitivity	55.3%	63.2%	52.6%	**73.7%**	60.5%	63.2%	65.8%	**84.2%**	56.7%	69.6%	57.4%	**75.6%**	54.6%	66.1%	**76.0%**	74.7%				
Specificity	51.3%	66.7%	**82.1%**	**82.1%**	56.4%	74.4%	82.1%	**84.6%**	56.9%	64.8%	76.2%	**81.5%**	64.3%	64.1%	76.8%	**80.5%**				
PPV	52.5%	64.9%	74.1%	**80.0%**	57.5%	70.6%	78.1%	**84.2%**	56.2%	65.8%	70.2%	**80.0%**	59.8%	64.2%	76.1%	**78.9%**				
NPV	54.1%	65.0%	64.0%	**76.2%**	59.5%	67.4%	71.1%	**84.6%**	57.4%	68.7%	64.7%	**77.4%**	59.2%	66.0%	**76.6%**	**76.6%**				

LOGOCV, leave-one-group-out cross-validation; NPV, negative predictive value; PPV, positive predictive value; SVM, support vector machine. Highest classification accuracy, sensitivity, specificity, NPV and PPV highlighted in bold for each data input and standardization method combination.

Table 3 Supervised learning ischaemic classification accuracies—analysing specific cardiac cycle intervals using the optimized reference pressure $P_{(aortic\ and\ distal)}$ as found in *Table 2*

Reference pressure	$P_{(aortic\ and\ distal)}$											
Classifier	**SVM**											
Data input	**Ensemble-average method**						**Individual cycle method**					
Standardization method	**Intra-vessel**			**Inter-vessel**			**Intra-vessel**			**Inter-vessel**		
Aortic pressure prediction interval	0–100%	0–100%	18–64%	0–100%	0–100%	18–64%	0–100%	0–100%	18–64%	0–100%	0–100%	18–64%
Distal pressure prediction interval	0–100%	18–64%	18–64%	0–100%	18–64%	18–64%	0–100%	18–64%	18–64%	0–100%	18–64%	18–64%
LOGOCV classification accuracy	77.9%	**81.8%**	79.2%	84.4%	**87.0%**	77.9%	78.7%	**79.8%**	79.1%	77.7%	**81.2%**	76.8%
Optimized GroupKFold mean classification accuracy (standard deviation)	77.8% (10%)	**81.8% (10.9%)**	79.2% (16.2%)	84.4% (15.3%)	**86.9% (14.4%)**	77.9% (16.5%)	78.6% (8.3%)	**79.6% (5.4%)**	79.0% (13.4%)	77.4% (19.1%)	**80.7% (5.8%)**	76.5% (10.7%)
Sensitivity	73.7%	**76.3%**	**76.3%**	84.2%	**86.8%**	81.6%	75.6%	**76.1%**	73.3%	74.7%	**81.2%**	75.1%
Specificity	82.1%	**87.2%**	82.1%	84.6%	**87.2%**	74.4%	81.5%	83.1%	**84.4%**	**80.5%**	**80.5%**	78.1%
PPV	80.0%	**85.3%**	80.6%	84.2%	**86.8%**	75.6%	80.0%	81.4%	**82.1%**	78.9%	**80.2%**	77.0%
NPV	76.2%	**79.1%**	78.0%	84.6%	**87.2%**	80.6%	77.4%	**78.1%**	76.5%	76.6%	**81.5%**	76.3%

LOGOCV, leave-one-group-out cross-validation; NPV, negative predictive value; PPV, positive predictive value; SVM, support vector machine. Highest classification accuracy, sensitivity, specificity, NPV and PPV highlighted in bold for each data input and standardization method combination.

Table 4 Supervised learning ischaemic classification accuracies—using the optimized prediction interval as found in *Table 3*

Number of pressure cycles	**15**											
Classifier	**SVM**											
Data input	**Ensemble-average method**						**Individual cycle method**					
Standardization method	**Intra-vessel**			**Inter-vessel**			**Intra-vessel**			**Inter-vessel**		
Reference pressure	P_{distal}	$P_{aortic–distal}$	$P_{aortic\ and\ distal}$	P_{distal}	$P_{aortic\ -\ distal}$	$P_{aortic\ and\ distal}$	P_{distal}	$P_{aortic–distal}$	$P_{aortic\ and\ distal}$	P_{distal}	$P_{aortic–distal}$	$P_{aortic\ and\ distal}$
Aortic pressure prediction interval	NA	18–64%	0–100%	NA	18–64%	0–100%	NA	18–64%	0–100%	NA	18–64%	0–100%
Distal pressure prediction interval	18–64%		18–64%	18–64%		18–64%	18–64%		18–64%	18–64%		18–64%
LOGOCV classification accuracy	62.3%	75.3%	**81.8%**	62.3%	75.3%	**87.0%**	65.6%	68.8%	**79.8%**	62.3%	80.0%	**81.2%**
Optimized GroupKFold mean classification accuracy (standard deviation)	62.5% (12.4%)	75.2% (8.0%)	**81.8% (10.9%)**	62.3% (15.3%)	75.3% 19.4%)	**86.9% (14.4%)**	65.3% (8.5%)	68.8% (4.7%)	**79.6% (5.4%)**	62.2% (13.3%)	80.1% (8.9%)	**80.7% (5.8%)**
Sensitivity	68.4%	63.2%	**76.3%**	63.2%	73.7%	**86.8%**	67.0%	70.7%	**76.1%**	50.5%	75.6%	**81.2%**
Specificity	56.4%	**87.2%**	**87.2%**	61.5%	76.9%	**87.2%**	63.4%	67.0%	**83.1%**	74.2%	**84.4%**	80.5%
PPV	60.5%	82.8%	**85.3%**	61.5%	75.7%	**86.8%**	64.1%	67.6%	**81.4%**	65.6%	**82.6%**	80.2%
NPV	64.7%	70.8%	**79.1%**	63.2%	75.0%	**87.2%**	66.4%	70.1%	**78.1%**	60.6%	78.0%	**81.5%**

LOGOCV, leave-one-group-out cross-validation; NPV, negative predictive value; PPV, positive predictive value; SVM, support vector machine. Highest classification accuracy, sensitivity, specificity, NPV and PPV highlighted in bold for each data input and standardization method combination.

whole-cycle $P_{(aortic)}$ data combined with an approximate diastolic interval of $P_{(distal)}$, highlighting the physiological principle of coronary perfusion occurring mostly during diastole. However, reduced accuracies when using this same diastolic interval for both proximal and distal pressures in $P_{(aortic\ and\ distal)}$ implies that central aortic pressure during systole does in fact impact coronary perfusion.

Analysing both inter- and intra-vessel standardization aimed to investigate whether ischaemia as labelled by FFR should be interpreted as a function of absolute pressure. That is, because FFR uses pressure as a surrogate for flow, but volumetric flux (flow rate) itself is a function of pressure, do identical FFR values between lesions truly reflect accurate oxygen delivery? Assuming identical systems, a pressure drop of 20% (equivalent to FFR of 0.8) at higher pressures would generate greater coronary flow compared with the same vessel and 20% pressure drop at lower absolute blood pressures. Therefore, does labelling a lesion as being significant based solely on pressure drop ignore critical information relating to the ability of the cardiac pump to generate perfusion pressure and provide sufficient flow? Intra-vessel standardization compares the shape of pressure waveforms between vessels without accounting for differences in their absolute blood pressures, whereas inter-vessel standardization compares both shape and relative blood pressures between all vessels being studied. Interestingly as shown in *Tables 2–4* when using whole-cycle $P_{(aortic\ and\ distal)}$, which yielded the highest accuracies (as shown in bold), inter-vessel standardization produced better classification accuracies in all cases except individual (non-ensembled) $P_{(aortic\ and\ distal)}$ waveforms. These differences which range from 0 to 6% suggest interpretation of FFR might in fact be improved when considered a function of blood pressure. Further sub-analysis regarding classification accuracies for blood pressure ranges was not performed.

Using the PCA Biplot, EigenCycles and absolute loading values heatmap (*Figure 2*) provides a novel method to investigate characteristics in the pressure waveforms that are most associated with ischaemia and provides insight into underlying physiology and could potentially contribute to future clinical practice.

PC 1 best separating ischaemic from non-ischaemic data (*Figure 2*) and its $P_{(aortic)}$ data having the darkest shading in the corresponding heatmap further supports whole-cycle aortic pressure data being important in dictating ischaemia. Since PC 1 by definition contributes most to overall variance and also best separates ischaemic from non-ischaemic data, this suggests that the overall shape/morphology of pressure waveforms (in addition to pressure itself) are an appropriate surrogate for ischaemia/flow. PC 4 separated ischaemia better than PC 3 and 2 even though it contributed less to overall variance. This implies slight differences in pressure values in certain sections of the waveform dictates identification of ischaemia. PC 4's largest loading values were from start of diastole in $P_{(distal)}$, implying subtle variations in coronary pressures at the start of diastole have significant effect on ischaemia. Finally, the darkest shades in any of the first four PC heatmaps occurred in data points 0–18 for PC 3 (peak systolic pressure to approximate end of systole), and 90–100 and 100–120 for PC 3 and 4, respectively (start of systole and early- to mid-systole, respectively), suggesting these intervals might be just as important as diastole in defining ischaemia and that $P_{(aortic)}$ heavily influences systolic coronary perfusion.

Limitations and advantages

We acknowledge limitations of this proof-of-concept study. Our study is a single-site study based on a relatively small data set, however, it provides hypothesis generation with a level of classification demonstrated comparable to established techniques. There was insufficient data to separate the analysis by coronary artery, which can be viewed as both a limitation and strength. Other studies have shown marked variation between the left and right coronary artery systems,[4] therefore, it is likely that our pooled artery results represent lower estimates of the techniques when compared with application in specific coronary branches. We also did not perform sub-analysis based on lesion types or plaque composition, which should be the topic of further work. It should also be noted that this study is based on baseline FFR measurements and study of hyperaemic responses will be the subject of ongoing research.

This is not an outcome study and instead should be interpreted as a comparison of ML to existing time-domain techniques that are considered validated, such as the numerical equivalence of RFR and dPR to iFR. A distinct advantage of ML approaches is the non-requirement to determine a numerical cut-off point to correspond to 'positivity' as is required for other NHPRs when comparing to FFR. Although the algorithm was trained using the accepted numeral cut-off for a positive FFR as a gold-standard, an ML approach provides a dichotomous result, positive or negative, with no 'grey zone'.

Impact on daily practice—clinical implications and interpretation

These results provide an application of ML to ischaemia. They employ a completely different approach to the usual time-domain averaging and as such could provide a useful support or adjudicator in equivocal cases. This algorithm is not proposed as a replacement for existing metrics since our results show the need for both $P_{(aortic)}$ and $P_{(distal)}$ data, but it can be derived without any extra data requirements.

Although FFR and some NHPRs are guideline indicated, other proposed NHPRs have been suggested and undergone various degrees of validation. This implies a general need for choice of technique in clinical practice. Machine learning techniques by providing a dichotomous result may be particularly useful as confirmatory evidence for clinical decisions in the so-called 'grey-zone' of other hyperaemic or non-hyperaemic indices.

Conclusion

Our ML algorithm when combining $P_{(aortic)}$ and $P_{(distal)}$ [$P_{(aortic\ and\ distal)}$] data under non-hyperaemic conditions is able to classify significant coronary lesions with accuracy similar to previous studies comparing various NHPRs to FFR. Further, there appear to be characteristics of coronary pressure waveforms identifiable by ML techniques that relate to function. These results provide an application of ML to ischaemia requiring only standard data from non-hyperaemic pressure measurements.

Supplementary material

Supplementary material is available at *European Heart Journal—Digital Health* online.

Funding

None declared.

Conflict of interest: None declared.

Data availability

The data underlying this article will not be shared publicly due to the privacy of individuals whose pressure waveforms were used in this study.

References

1. Lawton JS, Tamis-Holland JE, Bangalore S, Bates ER, Beckie TM, Bischoff JM, Bittl JA, Cohen MG, DiMaio JM, Don CW, Fremes SE, Gaudino MF, Goldberger ZD, Grant MC, Jaswal JB, Kurlansky PA, Mehran R, Metkus TS Jr, Nnacheta LC, Rao SV, Sellke FW, Sharma G, Yong CM, Zwischenberger BA. 2021 ACC/AHA/SCAI guideline for coronary artery revascularization: a report of the American college of cardiology/American heart association joint committee on clinical practice guidelines. *Circulation* 2022;**145**:e18–e114.
2. Van't Veer M, Pijls NHJ, Hennigan B, Watkins S, Ali ZA, De Bruyne B, Zimmermann FM, van Nunen LX, Barbato E, Berry C, Oldroyd KG. Comparison of different diastolic resting indexes to iFR: are they all equal? *J Am Coll Cardiol* 2017;**70**:3088–3096.
3. Johnson NP, Li W, Chen X, Hennigan B, Watkins S, Berry C, Fearon WF, Oldroyd KG. Diastolic pressure ratio: new approach and validation vs. the instantaneous wave-free ratio. *Eur Heart J* 2019;**40**:2585–2594.
4. Svanerud J, Ahn JM, Jeremias A, van 't Veer M, Gore A, Maehara A, Crowley A, Pijls NHJ, De Bruyne B, Johnson NP, Hennigan B, Watkins S, Berry C, Oldroyd KG, Park SJ, Ali ZA. Validation of a novel non-hyperaemic index of coronary artery stenosis severity: the resting full-cycle ratio (VALIDATE RFR) study. *EuroIntervention* 2018;**14**:806–814.
5. Götberg M, Christiansen EH, Gudmundsdottir IJ, Sandhall L, Danielewicz M, Jakobsen L, Olsson SE, Öhagen P, Olsson H, Omerovic E, Calais F, Lindroos P, Maeng M, Tödt T, Venetsanos D, James SK, Kåregren A, Nilsson M, Carlsson J, Hauer D, Jensen J, Karlsson AC, Panayi G, Erlinge D, Fröbert O. Instantaneous wave-free ratio versus fractional flow reserve to guide PCI. *N Engl J Med* 2017;**376**:1813–1823.
6. Sen S, Escaned J, Malik IS, Mikhail GW, Foale RA, Mila R, Tarkin J, Petraco R, Broyd C, Jabbour R, Sethi A, Baker CS, Bellamy M, Al-Bustami M, Hackett D, Khan M, Lefroy D, Parker KH, Hughes AD, Francis DP, Di Mario C, Mayet J, Davies JE. Development and validation of a new adenosine-independent index of stenosis severity from coronary wave-intensity analysis: results of the ADVISE (ADenosine vasodilator independent stenosis evaluation) study. *J Am Coll Cardiol* 2012;**59**:1392–1402.
7. Comella A, Chan JXW, Thakkar H, Michail M, Nicholls S, Gooley R, Ko B, Brown AJ. Agreement between iFR and other non-hyperaemic pressure ratios is not affected by severe aortic stenosis. *J Am Coll Cardiol* 2021;**77**:1061.
8. Jeremias A, Maehara A, Généreux P, Asrress KN, Berry C, De Bruyne B, Davies JE, Escaned J, Fearon WF, Gould KL, Johnson NP, Kirtane AJ, Koo BK, Marques KM, Nijjer S, Oldroyd KG, Petraco R, Piek JJ, Pijls NH, Redwood S, Siebes M, Spaan JAE, van 't Veer M, Mintz GS, Stone GW. Multicenter core laboratory comparison of the instantaneous wave-free ratio and resting P_d/P_a with fractional flow reserve: the RESOLVE study. *J Am Coll Cardiol* 2014;**63**:1253–1261.
9. Petraco R, Escaned J, Sen S, Nijjer S, Asrress KN, Echavarria-Pinto M, Lockie T, Khawaja MZ, Cuevas C, Foin N, Broyd C, Foale RA, Hadjiloizou N, Malik IS, Mikhail GW, Sethi A, Kaprielian R, Baker CS, Lefroy D, Bellamy M, Al-Bustami M, Khan MA, Hughes AD, Francis DP, Mayet J, Di Mario C, Redwood S, Davies JE. Classification performance of instantaneous wave-free ratio (iFR) and fractional flow reserve in a clinical population of intermediate coronary stenoses: results of the ADVISE registry. *EuroIntervention* 2013;**9**:91–101.